Transport-theory approach to ion-beam mixing and recoil implantation

Irwin Manning
Condensed Matter & Radiation Sciences Division, Naval Research Laboratory, Washington, D.C. 20375
(Received 27 June 1990)

Ion bombardment of an amorphous target in slab geometry is considered, and ion-beam mixing and recoil implantation evaluated in the binary-collision approximation. A fundamental equation for target-atom redistribution during ion bombardment is formulated, which relates the redistribution flux to the source function for the creation of energetic atomic recoils and their range distribution; for the analysis, this equation plays the role of the Boltzmann transport equation. Expanding the target-atom density in a power series and truncating at the second term yields a flux equation and closed expressions for coefficients of recoil implantation and of ion-beam mixing. The flux equation plays a role analogous to that of Fick's law in diffusion. Lattice relaxations are taken into account by introducing flux transformations between laboratory and marker coordinate frames. The closed expressions for the coefficients are calculated and compared with experiment. The binary-collision contribution to ion-beam mixing turns out to be larger than heretofore thought. A new mechanism for ion-beam mixing emerges, which turns out to make a very significant contribution. There are even cases where the new mechanism far outweighs the cascade-mixing mechanism, thought to be the major contributor to binary-collision ion-beam mixing.

When a solid target is bombarded by an energetic ion beam, the target atoms spatially redistribute themselves.[1] Beam-target collisions cause energetic recoils; the recoiling atom (primary knock-on atom or PKA) is itself an energetic ion traversing the target and goes on to generate a cascade of secondary knock-on atoms. The elastic collisions induced by the ion bombardment cause recoil implantation (RI), wherein target atoms are slammed downstream by collisions and ion-beam mixing (IM), a process resembling thermal diffusion but driven by collisions rather than thermal motions.[2] The binary-collision approximation is made throughout this paper, which assumes that these collisions involve only two-body interactions. Other major mechanisms of target-atom redistribution that have been identified include radiation-induced segregation, radiation-enhanced diffusion, and many-body effects (cascade spike effects) in ion-beam mixing, and these other mechanisms are thought to dominate over the simple binary-collision mechanism for ion-beam mixing.[1,3–5] However, in evaluating these other mechanisms it is essential that there be available a reliable calculation of the binary-collision mechanisms for IM and RI for the following two reasons: (1) In assessing redistribution experiments, the binary-collision contributions need to be subtracted off in order to estimate the size of the remaining effects, and (2) the binary-collision mechanisms are the fundamental forces driving these other mechanisms. This paper sketches a transport-theory approach, which, subject to certain restrictions, promises a realistic calculation of these binary-collision effects. The analysis is in the spirit of and employs the concepts of Boltzmann transport theory, but the fact is that the Boltzmann transport equation is not used in this analysis: Equation (1) below has in it all the information that will be required and, for the present analysis, serves the purpose of and replaces the Boltzmann transport equation.

Consider a beam of atomic species 1 bombarding, in slab geometry, an amorphous target consisting of atomic species 2 and 3. The beam is considered to be energetic enough that it comes to rest deep in the target, far beyond the region of interest. In the region of interest the beam is considered to be paraxial and monoenergetic. Consider a coordinate frame fixed to the deep interior of the target, far beyond the range of the bombarding ion beam, with the x axis perpendicular to the target surface, and let x_S be the x coordinate of the target surface, which is assumed not to vary with time. For the moment, focus attention on the redistribution flux J_3 of 3-atoms considered as a function of depth x; an expression for that quantity is found as follows.

One can write $dj_3 = N_3(x_3,t)S_3(\mathbf{v}_3)\,dx_3\,da$, where N_3 is the atomic density of 3-atoms at depth x_3 at time t, and dj_3 is the number of energetic 3-atom recoils created with velocity $\mathbf{v}_3$ at depth dx_3 about x_3 per unit area of the y-z plane per unit time, and in interval da about a, where a are a set of variables yet to be defined that determine $\mathbf{v}_3$. [An example of the variable set a will be given later in connection with Eq. (7) below.] The source function $S_3(\mathbf{v}_3)$ is defined by the above expression. For brevity, the variable t will often be omitted in writing $N_3(x,t)$ when that variable is not the focus of interest. Let $f(x;x_3,\mathbf{v}_3)$ be the range-distribution function for 3-atoms created at depth x_3 with velocity $\mathbf{v}_3$; such an atom has a probability $f\,dx$ of coming to rest at depth dx about x. This distribu-

tion function is to be taken as zero whenever x is outside the target; in our case $f = 0$ for $x < x_S$. Define the function F to be $F(x;x_3,\mathbf{v}_3) = \int_x^\infty dx' f(x';x_3,\mathbf{v}_3)$ for $x > x_3$ and $F(x;x_3,\mathbf{v}_3) = -\int_{x_S}^x dx' f(x';x_3,\mathbf{v}_3)$ for $x_S < x < x_3$. Using Gauss' law for conservation of particles, $\partial_x J_3(x) = -\partial_t N_3(x,t)$, one can show that, for x values inside the target ($x > x_S$), the flux J_3 is given by

$$J_3(x) = \int da\, S_3(\mathbf{v}_3) \int_{x_S}^\infty dx_3\, N_3(x_3,t) F(x;x_3,\mathbf{v}_3)\ . \tag{1}$$

Equation (1) is the basis of the present analysis.

An important role will be played by the operator $\mathcal{R}$ defined to be reflection with respect to the x axis: $\mathcal{R}\mathbf{v}_3$ is the vector that has an x component equal to $-v_{3x}$ and whose other components are the same as that of $\mathbf{v}_3$. One can always decompose the source function $S_3(\mathbf{v}_3)$ into a sum of parts that are even and odd with respect to this reflection: $S_3(\mathbf{v}_3) = S_3^e(\mathbf{v}_3) + S_3^o(\mathbf{v}_3)$, where $S^{e,o}(\mathbf{v}_3) \equiv \frac{1}{2}[S(\mathbf{v}_3) \pm S(\mathcal{R}\mathbf{v}_3)]$. A source function that is isotropic will be purely even; at the other extreme, a source function $S_3(\mathbf{v}_3)$ that is nonzero only for positive v_{3x} will have equal even and odd parts.

Expanding N_3 as a power series in x_3 about the (arbitrary) value x, substituting into Eq. (1), and truncating at the second term, one finds

$$J_3(x) = R_3 N_3(x,t) - D_3 \partial_x N_3(x,t)\ , \tag{2}$$

with

$$R_3 \equiv \int_{v_{3x}>0} da\, S_3^o(\mathbf{v}_3) M_1(\mathbf{v}_3)\ , \tag{3}$$

$$D_3 \equiv \int_{v_{3x}\geq 0} da\, S_3^e(\mathbf{v}_3) M_2(\mathbf{v}_3)\ , \tag{4}$$

and with the functions M_1 and M_2 defined to be $M_\mu(\mathbf{v}_3) \equiv \int_{-\infty}^\infty dx_3\,(x - x_3)^{\mu-1} F(x;x_3,\mathbf{v}_3)$. It turns out that, independent of the form of the range distribution $f(x;x_3,\mathbf{v}_3)$, $M_1 = x_R$ and $M_2 = \frac{1}{2}(x_R^2 + \sigma_R^2)$, where $x_R(\mathbf{v}_3)$ is the projected range (projected on the x axis) of an energetic 3-atom created with velocity $\mathbf{v}_3$ and $\sigma_R(\mathbf{v}_3)$ is its straggling in projected range. It is significant that the coefficient R_3 depends only on the odd part of $S_3(\mathbf{v}_3)$ and D_3 depends only on the even part of $S_3(\mathbf{v}_3)$. A similar analysis yields expressions for the flux $J_2(x)$ of 2-atoms analogous to those of Eqs. (2), (3), and (4) above. Having expanded N_3 in a power series in x, the coefficients R_3 and D_3 of Eqs. (3) and (4) are spatially independent and do not involve the variable x; these equations now consider the target to be homogeneous. Correspondingly, we must now set $x_R = -\infty$ in the evaluation of R_3 and D_3. These expressions for R and D will be discussed, but first let us pause to examine the flux equation (2).

Suppose that at time $t = 0$ the atomic density N_3 is given by $N_3(x,0) = \delta(x)$, where δ is the Dirac δ function. Then one can show that the solution of Eq. (2) is $N_3(x,t) = G(x,t)$, where G(x,t) is the familiar Gaussian function describing ordinary diffusion for this initial condition, with standard deviation $\sigma = \sqrt{2D_3 t}$, but centered at the plane $x = R_3 t$. The solution G is thus the Gaussian describing ordinary diffusion, but drifting to the right with velocity R_3. Also note that, if $R_3 = 0$, Eq. (2) is just Fick's law for diffusion. Thus, there is a clean separation between drift and broadening effects in the two terms of Eq. (2). This separation prompts us to propose a different usage of the terms *recoil implantation* and *mixing* than that often employed: In this paper the effects of the first term of Eq. (2) will be referred to as recoil implantation, and the effects of the second term will be referred to as ion-beam mixing. Because of the linearity of Eq. (2), the function G is a Green's function for that equation: For N_3 an arbitrary function $N_3(x,0)$ at $t = 0$, one has $N_3(x,t) = \int_{-\infty}^\infty dx'\, G(x-x',t) N_3(x',0)$. Thus, for any experimental configuration (in slab geometry), the flux Eq. (2) determines $N_3(x,t)$ for all subsequent times from its value at $t = 0$.

The derivation of the flux equation (2) relied on the important approximation that the power series expansion of N_3 can be truncated at the second term. The sweeping implications of this approximation must be emphasized. To begin with, this approximation can only be valid when individual collisions do not make abrupt changes in N_3; in this approximation the changes in N_3 are due to the cumulative effect of many collisions, with each individual collision changing N_3 infinitesmally. In addition, the requirement that this power series can be truncated at the second term is roughly equivalent to requiring that $\partial_x N_3 << N_3$; in the Gaussian Green's function $G(x,t)$ this is equivalent to requiring, for the standard deviation σ, that the time t be sufficiently large that

$$\sigma/\lambda \gg 1\ , \tag{5}$$

where λ is the largest significant mean-free path between collisions.

During the ion bombardment different parts of the target will expand and contract because of atomic redistributions, and the above discussion of the flux equation (2) must be altered to take account of these lattice relaxations, which can be done in the following manner: Let the *laboratory frame* be the coordinate frame defined in connection with Eq. (1), that is to say, a coordinate frame fixed to the deep interior of the target, and let the *marker frame* be the coordinate frame of that name employed by Darken in his analysis of the Kirkendall effect.[6] To the extent that a lattice plane maintains its integrity during bombardment, the marker frame can be thought of as a coordinate frame fixed to a particular lattice plane perpendicular to the x axis. The marker frame moves with respect to the laboratory frame, and, in general, there is a different marker frame for each different value of target depth x. Because of this motion, the flux J_i of target atoms of atomic species i will be different in the two coordinate frames. Let $v_M(x)$ be the velocity of the marker frame at depth x with respect to the laboratory

frame. The fluxes seen in the two frames are related by the flux transformation $J_{iM}(x) = J_{iL}(x) + v_M(x)N_i(x)$ for atomic species $i = 2, 3$, where the subscripts M and L denote the marker and laboratory frames. The flux Eq. (2) is valid in the marker frame. In order to evaluate experimental results, one must transform this equation to the laboratory frame, which can be done as follows.

One must know how the target density varies with varying concentrations of the constituent atomic species; for this purpose we will assume that the target obeys Vegard's law $\sum_{i=1}^{3} \omega_i N_i(x) = 1$, where ω_i is the atomic volume of an atom of species i.[7] Using Gauss' law for conservation of particles, one can show that this implies $\sum_{i=1}^{3} \omega_i J_{iL}(x) = 0$. Using this result together with the flux transformation equation above to first determine $v_M(x)$ and then to transform the flux equation (2) from the marker frame to the laboratory frame, one finds

$$J_{3L}(x) = [R_3 - R_2 - \omega_1 J_1 + \omega_3 N_3 (R_2 - R_3)]N_3 - [D_3 + (D_2 - D_3)\omega_3 N_3]\partial_x N_3 , \quad (6)$$

where J_1 is the bombarding-beam flux. We will assume that the atomic concentration of 3-atoms is small. In the flux equation (6) one can then drop the terms that contain the factor $w_3 N_3$, and this equation now becomes linear, similar to the flux equation (2) and with a similar Green's-function solution, but this time with drift velocity given by $R_3 - R_2 - \omega_1 J_1$ rather than by R_3.

In general, the surface will move with respect to the laboratory frame because of sputtering and, as in ion-beam-aided deposition, adsorption. The above discussion of J_{3L} remains unchanged in this case, provided we retain the assumption of monoenergetic paraxial penetrating beam. However, when this assumption is relaxed, as when discussing implantation-profile evolution in time during ion bombardment, then a third coordinate frame becomes cogent: The *target frame*, defined to be a coordinate frame moving such that the target surface is always located at the origin. The above analysis can be used as a starting point to address this profile time evolution in the presence of lattice relaxation, but that is not done in the present work.

Let us now return to the discussion of the coefficients R_3 and D_3 of Eqs. (3) and (4). Corresponding to the fact that energetic 3-atoms are created in collisions in which a 1-, 2-, or 3-atom collides with a 3-atom at rest, the source function $S_3(\mathbf{v}_3)$ is a sum of three terms: $S_3 = S_3^{13} + S_3^{23} + S_3^{33}$. The assumption that the concentration N_3 of 3-atoms is small significantly simplifies the calculation of R_3 and D_3 by allowing one to ignore the 3-3 collisions and drop the S_3^{33} term. (The calculation of these quantities can be done without this simplification.) Corresponding to the source function S_3 now being a sum of two terms, one has $D_3 = D_3^{13} + D_3^{23}$, and a similar sum for R_3. Similar observations apply to the calculation of R_2 and D_2, where one can write $D_2 = D_2^{12} + D_2^{22}$.

Consider now the calculation of D_3^{23}. Let ψ_2 be the single-particle distribution function for steady-state production of energetic 2-atoms during the ion bombardment: $\psi_2(\mathbf{v}_2)\, d^3v_2$ is the number of 2-atoms with velocity in d^3v_2 about $\mathbf{v}_2$. For the variable set a, which determines $\mathbf{v}_3$ in Eq. (1), choose $\mathbf{v}_2$, $\cos\chi$, and β, where χ is the center-of-mass scattering angle in a 2-3 collision, and β is the azimuthal angle for that collision. (The velocities are in the laboratory frame; the angles are in the center-of-mass frame.) Define the quantity K_{23} by saying that the cross section for a 2-3 collision is given by $N_3 K_{23}\, d(\cos\chi)\, d\beta$. One can show that Eq. (4) for D gives

$$D_3^{23} = \int d^3v_2\, d(\cos\chi)\, d\beta\, K_{23} v_2 \psi_2^e(\mathbf{v}_2) M_2(\mathbf{v}_3) . \quad (7)$$

The recoil-implantation parameter R_3^{23} has a similar expression, but with ψ_2^e instead of ψ_2^e and with M_1 instead of M_2. It is significant that D depends only on the even part of ψ_2, and R depends only on the odd part of ψ_2. The physical mechanism for IM expressed by D_3^{23} of Eq. (7) is that of cascade mixing, which is the Einstein picture of gaseous diffusion as extended to ion bombardment by Haff and Switkowsky.[8] According to this picture the flux $J_3(x)$ is the algebraic sum of positive and negative contributions which are equal and opposite unless N_3 is spatially varying, in which case this algebraic sum is proportional to the gradient of N_3.

Similarly, for the contribution from 1-3 collisions one finds

$$D_3^{13} = J_1 \int d(\cos\chi)\, d\beta\, K_{13} M_2(\mathbf{v}_3) , \quad (8)$$

with a similar expression for R_3^{13}, but with M_1 instead of M_2. The ion-beam mixing D_3^{13} caused by 1-3 collisions involves a different mechanism than the cascade-mixing mechanism D_3^{23} caused by 2-3 collisions. In contrast to the situation in the D_3^{23} of Eq. (7), where all of the atoms incident on and colliding with the target 3-atom have the slab-geometry analog of isotropic velocity distributions, all of the incident atoms in the D_3^{13} of Eq. (8) are moving downstream (in the marker frame). We will see later, in Table II, that this 1-3 mechanism, surprisingly, contributes very significantly to IM. If N_3 is spatially constant, this gives rise to the flux $R_3^{13} N_3$ of the first term of the flux Eq. (2). If N_3 is spatially varying, then the flux seen at the plane x must be corrected for the fact that the 3-atom density at the creation site is different than $N_3(x)$; this correction leads to the second term of the flux Eq. (2). The condition Eq. (5) implies that the sum of these two terms will always be positive; J_3^{13} is always pointed downstream (in the marker frame), but in such a way that the Green's function $G_3^{13}(x,t)$ for the solution of the 1-3 flux equation for J_3^{13} is that discussed in the paragraph above containing Eq. (5), with a downstream drift (in the marker frame) determined by R_3^{13} and a broadening (in the marker frame) determined by D_3^{13}.

To calculate D_3^{23} and R_3^{23} one must be able to evaluate the steady-state distribution function $\psi_2(\mathbf{v}_2)$, which

TABLE I. Comparison of the present calculation of the ion-beam mixing parameter D_3 with the data of Ref. 14.

Z_1	$\frac{1}{J_1}D_3$ (10^3 Å^4)			
Z_3	50-keV Ne	110-keV Ar	220-keV Kr	300-keV Xe
Ni expt.	0.12±0.04	0.6±0.2	1.7±0.2	3.7±1
calc.	0.334	1.30	5.46	10.7
Ge expt.	0.9±0.3	1.4±0.5	4.8±0.8	8.8±1.4
calc.	0.277	1.06	4.54	9.18
Sn expt.	0.9±0.3	1.8±0.6	4.3±0.9	5.5±0.8
calc.	0.217	0.766	3.21	6.68
Sb expt.	0.7±0.3	1.7±0.6	4.1±1	5.9±0.8
calc.	0.213	0.747	3.31	7.08
Pt expt.	0.7±0.3	1.4±0.5	3.4±0.9	4.1±1
calc.	0.170	0.599	2.55	5.62
Au expt.	1.3±0.5	2.7±1	7.3±1.5	8.2±1
calc.	0.161	0.563	2.42	5.46

was done by employing the Monte Carlo computer code TRIMCAS,[9] modified to evaluate this quantity. The sister code TRIM2D was used to obtain the range parameters needed for M_1 and M_2.[10] These two codes used the universal interatomic potential described in Ref. 11 for elastic collisions, and both codes were modified so that inelastic (electronic) stopping was that of Lindhard-Scharff-Schiott (LSS) with a k value given by Ref. 12.[13] In all of the calculations about to be described, a vacancy was not produced unless the target atom was given an energy of at least E_d, in which case the recoiling atom has as energy the transferred energy less E_b; all the calculations here used E_d =14 eV and E_b =0.5 eV. Let $N_3 = 0$ and $\partial_x N_2 = 0$, in which case the version of the flux Eq. (2) for J_2 gives (exactly) $\int d^3v_2\, \mathbf{v}_2 \psi_2(\mathbf{v}_2) = R_2 N_2$. Actually, this equation can be considered the sum of two equations for recoiling 2-atoms created by, respectively, 1-2 and 2-2 collisions. In the equation involving R_2^{12} the contribution to $\psi_2(\mathbf{v}_2)$ is from PKA's only, while the contribution to $\psi_2(\mathbf{v}_2)$ in the equation involving R_2^{22} is from secondary knock-on atoms only. These two equations constitute two sum rules that must be exactly satisfied by any self-consistent calculation. For the case of Figs. (1) and (2): the sum rule for R_2^{12} was satisfied with 5.1% error and the sum rule for R_2^{22} was satisfied with 2.0% error, which are consistent with the Monte Carlo fluctuations in the calculation of $\psi_2(\mathbf{v}_2)$. (In all of the TRIMCAS calculations of this paper, the number of histories was chosen to produce about four million vacancies per run.)

To compare the above expressions with experiment, consider as a typical case the data of Ref. 14, where Z_2 is silicon. In these experiments, the targets were all initially prepared as thin layers of 3-atom material sandwiched between 2-atom material. Our assumption that N_3 is small is violated here and, equally serious, it will turn out that the requirement of Eq. (5) is also violated, so comparison with experiment cannot properly be made. Comparison could be made in an experiment in which the target is bombarded long enough so that σ of Eq. (5) is sufficiently large, the target then taken out, measured, returned for another bombardment, and taken out and measured again. Nevertheless, it is of interest to compare the data of Ref. 14 with the present calculation, which is done in Table I. This table indicates that binary collisions make a larger contribution to ion-beam mixing than heretofore thought.[4,5] Table II indicates that the 1-3 collision mechanism makes a very significant contribution to IM. There are even cases where this contribution far outweighs the contribution from the (cascade-mixing mechanism) 2-3 collisions. This is a surprise because the incident atoms in 1-3 collisions are all moving in the forward direction (in the marker frame). One would expect

TABLE II. The recoil implantation mixing parameter R_3 and the fractional contribution of 2-3 collisions to the ion-beam mixing parameter D_3 for two representative 3-atoms.

Z_1	50-keV Ne	110-keV Ar	220-keV Kr	300-keV Xe
Z_3				
		D_3^{23}/D_3 (%)		
Ge	46.2	34.4	20.8	17.4
Pt	41.1	32.7	22.0	16.8
		$\frac{1}{J_1}R_3$ (10Å^3)		
Ge	0.813	1.56	3.53	6.03
Pt	0.774	1.42	3.23	5.36

these collisions to make a small contribution to IM in comparison with the 2-3 collisions, where the incident atoms are more isotropic. In the calculations for the two tables, the energy used for the beam was not the actual beam energy listed in the Z_1 row but a lower value corresponding to the energy degradation the beam suffers in traversing the target to get at the 3-atom layer. For the Ni, Ge, and Sn targets the energies used were 31.6, 72.4, 145, and 187 keV, respectively, while for the Sb, Pt, and Au targets, the energies used were 40.8, 91.2, 183, and 243 keV, respectively.

In the expressions for D_3, Eqs. (7) and (8), imagine that the integrations are arranged so that an integration $\int_{E_3}^{E_{3\,\max}} dE_3'$ is done last, where E_3' is the energy of a 3-atom recoil at creation, and consider D_3 to be a function of the lower limit of integration E_3. These functions for D_3^{13} and D_3^{23} are depicted in Fig. 1 for the case of Z_1 = Ar and Z_3 = Ge of Tables I and II, along with the corresponding functions of R_3, as well as the projected range x_P of 3-recoils as a function of E_3 for $\mathbf{v}_3$ parallel to the x axis. The experimental data of Ref. 14 imply that in this case σ of Eq. (5) was 91.7 Å. Figure 1 shows that 96% of the contribution by D^{13} to IM and 66% of the contribution by D^{23} involves 3-atom ranges x_P larger than this value, which is why comparisons of the present calculation to those data are not properly valid.

Now imagine that the integrations for R_3^{23} and D_3^{23} are arranged so that an integration $\int_{E_2}^{E_{2\,\max}} dE_2'$ is done last, where E_2' is the energy of the 2-atom incident on the 3-atom in a 2-3 collision; Fig. 2 shows D_3^{23} and R_3^{23} considered as functions of the lower limit of integration E_2. Here one finds that 88% of the contribution by D^{23} to IM comes from E_2 energies involving 2-atom ranges x_P larger than the value of σ.

The high-energy contributions in Figs. 1 and 2 come mainly from large-excursion events that probably would not satisfy the power-series approximation leading to Eq. (2). The big role played by these high-energy contributions raises the question of to what extent these large-excursion events should be included in the calculations of R and D and, equally important, to what extent they are included in the reported experimental measurements of R and D. This is an important point requiring further investigation.

It would be of interest to relax the condition of Eq. (5) and the condition that N_3 be small by avoiding the power-series expansion of $N_3(x_3)$ by dealing directly with Eq. (1) and by dealing with the resulting nonlinear laboratory-frame flux corresponding to Eq. (6). At least for the 1-3 contribution, it should be feasible to numerically evaluate Eq. (1) combined with numerical integration of the laboratory-frame flux corresponding to Eq.

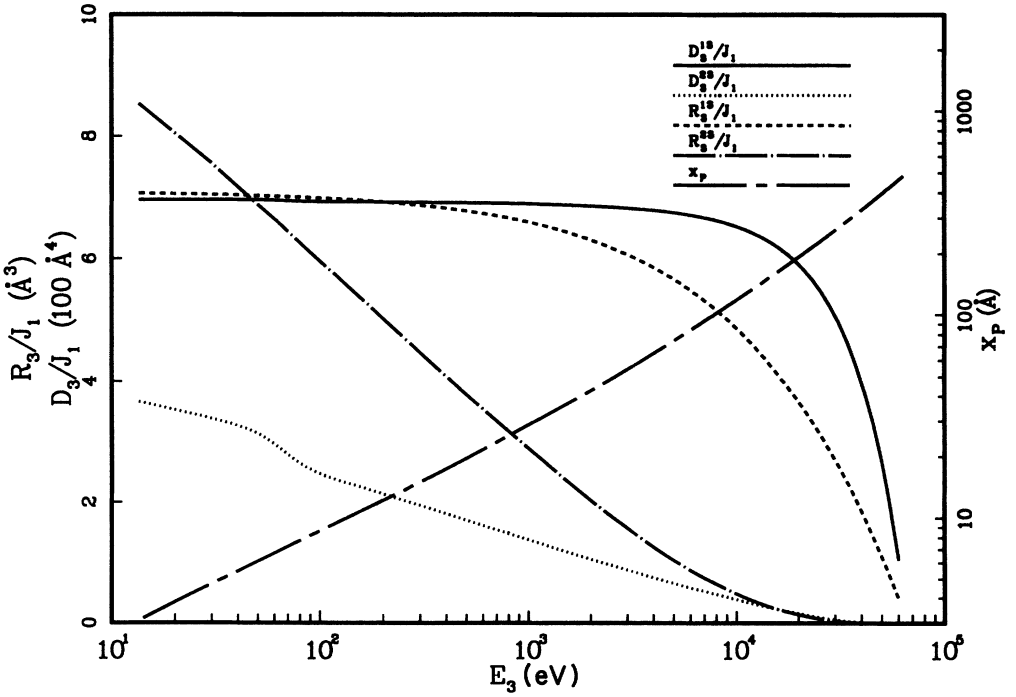

FIG. 1. Ion-mixing parameters D_3 and recoil-implantation parameters R_3 for 1-3 and 2-3 collisions, considered as a function of the lower limit of integration E_3, the 3-atom recoil energy. The projected range x_P of 3-atoms as a function of E_3 is also shown for $\mathbf{v}_3$ parallel to the x axis. The case depicted is that of Z_1 = 72.4-keV Ar, Z_2 =Si, and Z_3 =Ge.

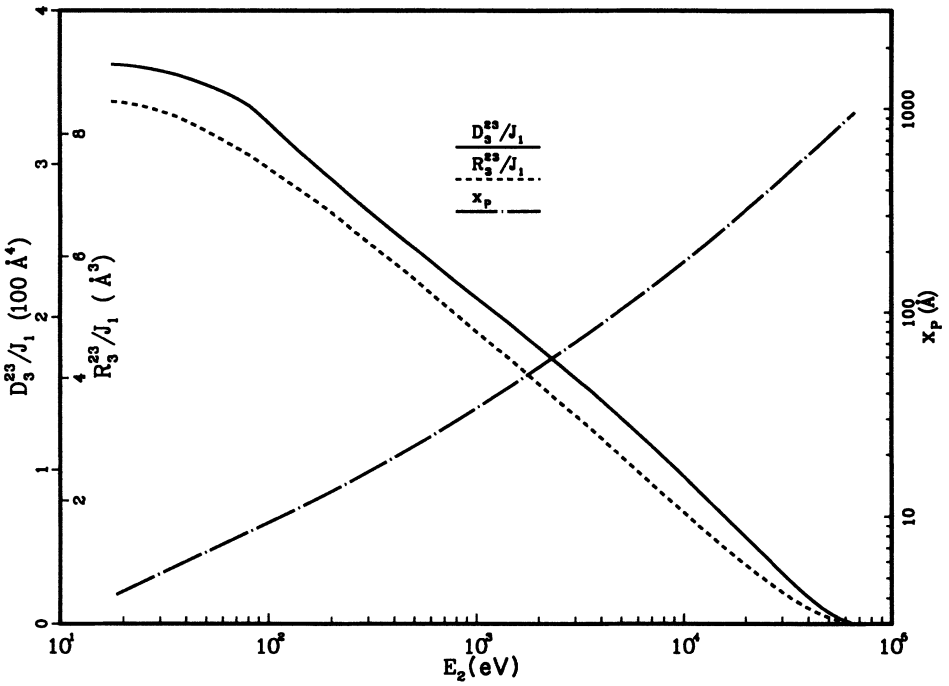

FIG. 2. Ion-mixing parameter D_3^{23} and recoil implantation parameter R_3^{23} for 2-3 collisions, considered as a function of the lower limit of integration E_2, the 2-atom incident energy. The projected range x_P of 2-atoms as a function of E_2 is also shown for $\mathbf{v}_2$ parallel to the x axis. This is the same case as in Fig. 1.

(6).

The dependence of IM and RI on the displacement energy E_{d2} for 2-atoms and E_{d3} for 3-atoms is of interest because a strong dependence on E_d would imply a strong binary-collision contribution to chemical, beam fluence, density, and temperature effects in IM and RI. Figure 2 shows that there will be very little dependence on E_{d2}, but Fig. 1 indicates a strong dependence of R_3^{23} and a moderate dependence of D_3^{23} on E_{d3}. Correspondingly, we can expect a fairly strong dependence of R_3 and a rather weak dependence of D_3 on E_{d3}.

Table II also shows calculated values of R_3 for two typical targets of the data of Ref. 14. Recoil implantation was not measured in that work, but data for two cases of RI is available in Ref. 15. There, for Z_1 =300 keV Xe, Z_2 =Si, and Z_3 =Pt, the measured R/J_1 was 110±50 Å^3; the corresponding calculated values turn out to be R_3/J_1 =62.6 Å^3 and R_2/J_1 =71.7 Å^3, which would predict a negative drift rather than the positive drift observed. Similar results were obtained for the other case of Ref. 15. Negative drifts were also found by Littmark.[2] If, as seems likely, this disagreement between experiment and the present calculation were to persist after a proper comparison was possible, then the discrepancy would have to be attributed to some mechanism other that of binary collisions, such as radiation-induced segregation.

[1]S.M. Myers, Nucl. Instrum. Methods **168**, 265 (1980).
[2]Existing theoretical approaches to evaluating the binary-collision contributions to target-atom redistributions, notably the works of Sigmund, Gras-Marti, and Littmark, are reviewed in U. Littmark, Nucl. Instrum. Methods B **7/8**, 684 (1985).
[3]L. E. Rehn, Mater. Res. Soc. Symp. Proc. **7**, 17 (1982).
[4]R. S. Averbach, Nucl. Instrum. Methods B **15**, 675 (1986).
[5]L. Rehn and P. Okamoto, Nucl. Instrum. Methods B **39**, 104 (1989).
[6]L. Darken, Trans. AIME **174**, 125 (1948). The marker frame is well described in P. G. Shewmon, *Diffusion in Solids* (McGraw-Hill, New York, 1963), Chap. 4.
[7]K. A. Geschneider and G. H. Vineyard, J. Appl. Phys. **33**, 3444 (1962).
[8]P. K. Haff and Z. E. Switkowski, J. Appl. Phys. **48**, 3383 (1977).
[9]J. P. Biersack and W. Eckstein, Appl. Phys. A **34**, 73 (1984).
[10]J. P. Biersack and L. G. Haggmark, Nucl. Instrum. Methods **174**, 257 (1980).
[11]J. F. Ziegler, J. P. Biersack, and U. Littmark, *The Stopping and Range of Ions in Solids*, Vol. 1 of *The Stopping and Ranges of Ions in Matter* (Pergamon, New York, 1985).
[12]D. J. Land and J. G. Brennan, At. Data Nucl. Data Tables **22**, 235 (1978).
[13]I. Manning, Nucl. Instrum. Methods (to be published).
[14]S. Matteson *et al.*, Nucl. Instrum. Methods **182/183**, 43 (1981).
[15]B. M. Paine and M-A. Nicolet, Nucl. Instrum. Methods **209/210**, 173 (1983).